Characterization of an electrochemical pilot plant filterpress reactor by hydrodynamic and mass transport studies

ARTICLE · JANUARY 2000

Source: OAI

7 AUTHORS, INCLUDING:

Ángel Frías Ferrer
University of Alicante
32 PUBLICATIONS **628** CITATIONS

SEE PROFILE

Juan A. Conesa
University of Alicante
130 PUBLICATIONS **3,128** CITATIONS

SEE PROFILE

KINETICS, CATALYSIS, AND REACTION ENGINEERING

Characterization of an Electrochemical Pilot-Plant Filter-Press Reactor by Hydrodynamic and Mass Transport Studies

José González-García, Angel Frías, Eduardo Expósito, Vicente Montiel,* and Antonio Aldaz

Grupo de Electroquímica Aplicada, Departamento de Química Física, Universidad de Alicante, Ap. Correos 99, 03080 Alicante, Spain

Juan A. Conesa

Departamento de Ingeniería Química, Universidad de Alicante, Ap. Correos 99, 03080 Alicante, Spain

This work deals with the study of the influence of turbulence promoters in the hydrodynamic and mass transport behavior of a pilot-plant filter-press electrolyzer (a homemade UA200.08 with a 200 cm^2 electrode area) in an undivided configuration. A simple experimental arrangement was used to generate data from electrolytic conductivity measurements in a series of impulse−response experiments. The presence and type of turbulence promoters influence the flow distribution inside the reactor. A new design of a model (presented in a previous work) has been used to analyze the residence time distributions. In this study a new parameter, the turbulence factor, given as $N_\alpha\Phi_\beta$, was employed to classify the turbulence promoters. The optimization of the parameters indicates that the correct model is dispersed plug-flow behavior with a low axial dispersion that considers exchange between the dead and main zones of the reactor. It is also very interesting to highlight that the information obtained by means of the turbulence factors is similar to that obtained from the values of the mass transport coefficients measured using the limiting current technique.

1. Introduction

Filter-press-type electrolyzers are one of the most important electrochemical reactors.[1] The parallel-plate configuration is widely used because of its numerous attractive characteristics. These advantages can be seen from an industrial, research, or practical point of view: wide availability of its components;[2] ease of scale-up[3,4] and versatility,[5] which enables the electrolyzers to be used in different configurations for a wide variety of processes; growth in the successful application of pilot- and full-scale electrochemical filter-press reactors;[6−8] wide offer of commercial electrochemical filter-press reactors from laboratory to industrial scale;[9,10] simplicity of construction;[11] uniform potential distribution;[12] ease of operation and minimal maintenance problems;[13] possibility of electrical monopolar or bipolar connection;[14,15] incorporation of three-dimensional electrodes;[16] incorporation of turbulence promoters;[17] and ease of gas removal[18,19] and of temperature and flow control.[20]

These advantageous characteristics make the filter-press configuration one of the most studied in the academic field.[21−25] A special interest has been taken in the incorporation of turbulence promoters, studying the influence in the mass transport to the electrode with electrochemical techniques.[26−29] Nevertheless, the hydrodynamic behavior of such systems has not been widely studied, although some papers have appeared recently. Techniques usually used are flow visualization[30,31] and modeling of the residence time distribution (RTD).[32−34]

In this paper, a study of a pilot-plant electrochemical filter-press cell (a homemade UA200.08 reactor) is described, analyzing the influence of turbulence promoters on the hydrodynamic and mass transport behavior. A new design of a model recently developed to analyze the different RTDs[35] is tested in this new reactor. The turbulence factor, introduced in that paper, has been used to classify the effectiveness of the turbulence promoters, and the results have been compared with those obtained with the limiting current technique from electrochemical methods. Furthermore, the characterization of a family of homemade reactors has been done. These reactors have been used in electro-organic synthesis processes that have been scaled to industrial scale.[3−5] On the other hand, the family of reactors is formed by a laboratory-scale reactor UA63.03, a bench-scale reactor UA200.08, and a pilot-plant reactor UA1000, with a scale factor of ≈4 in the scaling of the electrode area. The information obtained has been used to produce the commercially available reactors REIM 2500 and REIM 3300 supplied by "I. D. Electroquímica".

2. Experimental Section

The electrochemical reactor was a homemade filter-press electrochemical cell (UA200.08). Details such as a view of the compartment, an exploded view of the reactor, and its geometrical dimensions are shown in Figure 1 (taken from ref 36). The turbulence promoters

* To whom correspondence should be addressed. E-mail: vicente.montiel@ua.es.

10.1021/ie990351q CCC: $19.00
Published on Web 04/08/2000

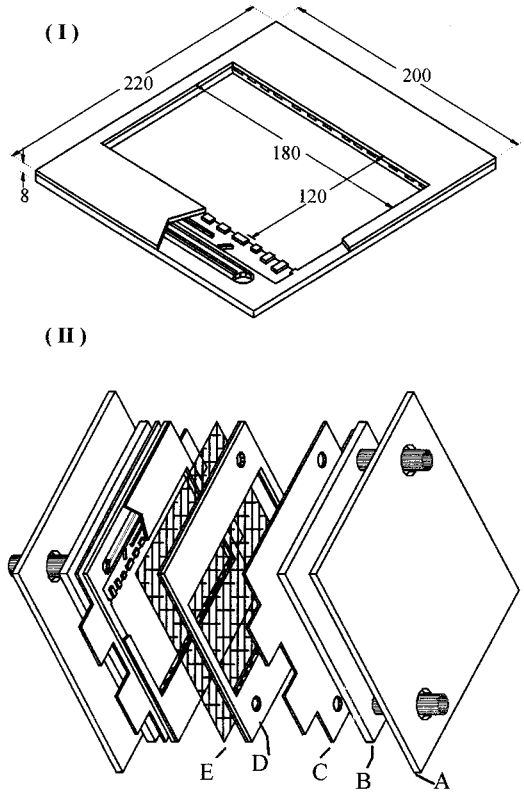

Figure 1. (I) View of a compartment (or chamber) showing details of flow distributors and geometric dimensions (mm). (II) Exploded view of the UA200.08 reactor in the divided mode showing the (A) backplate, (B) polypropylene block with flow channels, (C) flat plate, (D) compartment (or chamber), and (E) separator.

used were very similar to those used in other works found in the literature, and its geometrical dimensions and view are shown in Figure 2 and Table 1. It is interesting to point out the characteristics of the turbulence promoters, such as the strands, apertures, and mesh area, which are important aspects in the full characterization of the turbulence promoters.

The promoters were placed in the compartment and were joined together, with the long diagonal parallel to the flow direction (when working with promoter C also with the short diagonal). The number of promoters was high enough to ensure that, after being tightened, the compartment is completely occupied and the promoters cannot be moved away.

The pressure drop measurements and RTD experiments were carried out using the same apparatus and experimental technique presented in the previous work.[36] The electrolyte used for the pressure drop measurements was a 0.5 M sodium sulfate solution. Water was used for RTD experiments. A KCl-saturated solution was used as the tracer.

The mass transport study was carried out using the limiting current technique. The working and counter electrodes were copper plates. To determine the correcting factor (see the Mass Transport Study Section), partially active electrodes were used. These partially active electrodes presented a 4-cm-length film of nonconducting polymer at the margins. An saturated calomel electrode (SCE) was used as the reference electrode. The test reaction was the cathodic reduction of Cu(II) in a 0.5 M sodium sulfate solution. The experiments were carried out as a function of the copper(II) concentration (lower than 60 ppm) and the

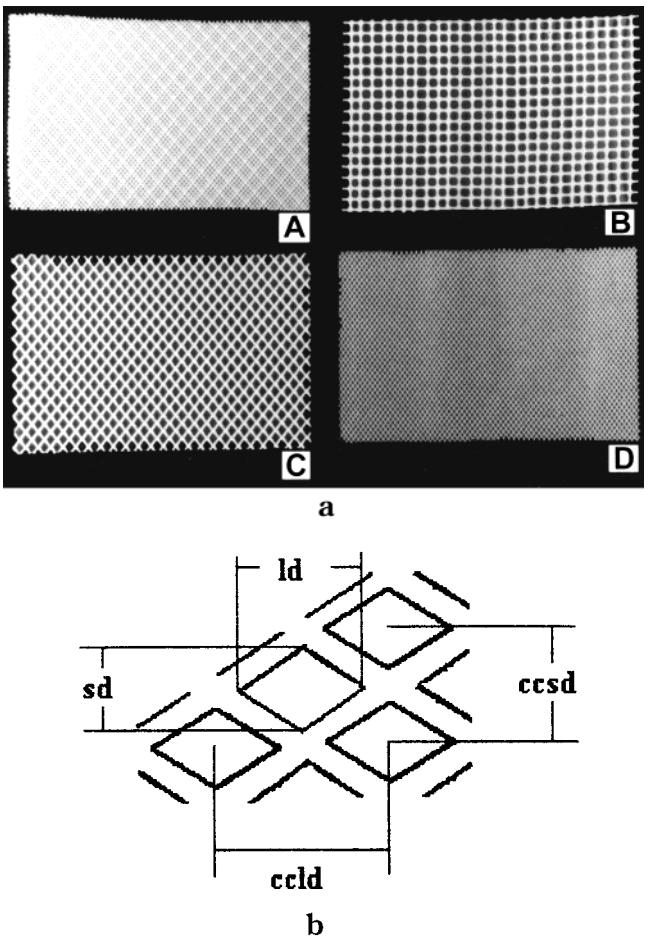

Figure 2. (a) Turbulence promoters used during the study. (b) Sketch of the parameters of the turbulence promoters (values in Table 1).

Table 1. Characteristic Dimensions for the Turbulence Promoters[a]

	type of promoter			
	A	B	C	D
sd/mm	1.5	5−7*	5	2
ld/mm	2	5−7*	6	3
ccld/mm	3.1	6.2	8.7	3.7
ccsd/mm	2.3	6.2	6.6	2.4
promoter thickness/mm	1	1	2	1
FT/mm	0.5	0.9	1.2	0.6
porosity	0.69	0.70	0.73	0.77

[a] Asterisk indicates the side of a square. sd is the short diagonal, ld is the long diagonal, ccsd is the distance between the center of a promoter gap and the center of the next closest gap in the ld direction, ccsd is the distance between the center of a promoter gap and the center of the next closest gap in the sd direction and FT is the fiber porosity.

flow conditions (*Re* between 90 and 800) both with and without turbulence promoters in the electrolyte flow.

Current vs potential curves were recorded by scanning from the rest potential to the hydrogen-evolving potential (−800 mV vs SCE) at 1−5 mV s^{-1}. A typical polarization curve is shown in Figure 3. All of the responses showed a well-defined limiting current plateau extending from −200 to −800 mV vs SCE, where a hydrogen-evolving reaction was observed. However, the limiting currents were measured by means of the potential step experiments from the rest potential to the mass transport control region (−500 mV vs SCE) where the value of the current is constant with time.

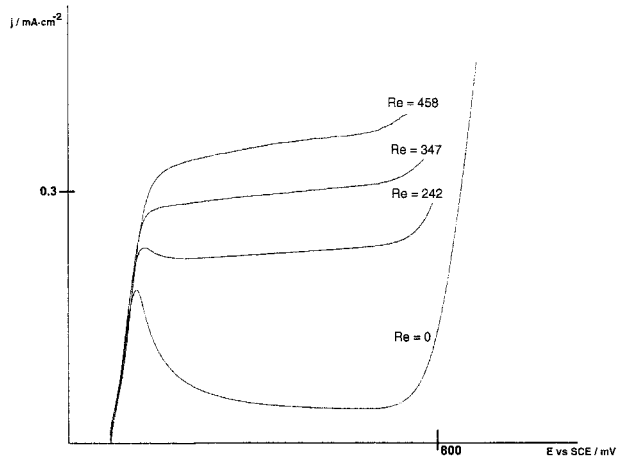

Figure 3. Typical polarization curve for the system. [Cu^{2+}] = 60 ppm.

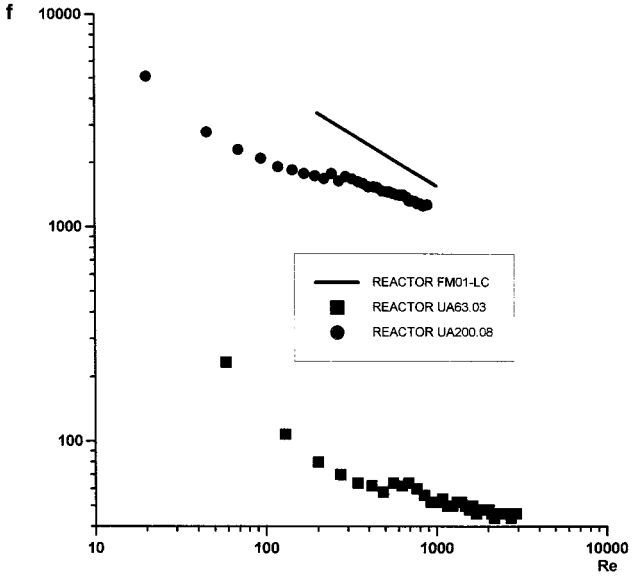

Figure 4. Double logarithmic plot of the friction factor vs Reynolds number for the reactor UA63.03,[35] reactor UA200.08 (present study), and FM01-LC electrolyzer of ICI.[37]

3. Results

3.1. Hydrodynamic Study. 3.1.1. Pressure Drop Measurements. Pressure drop data are reported in order to determine the laminar and turbulent flow patterns. In a well-defined channel flow, the transition from laminar to turbulent flow occurs at around $Re = 2000$[20] ($=vd_e/\nu$). This result refers to experimental conditions which are usually achieved by a deliberate calming section, to obtain fully developed laminar or turbulent flow as a function of the *Re* number. In practical reactors, there is no calming section and the manifolds directly inject or extract the electrolyte in the interelectrode channel.

Figure 4 compares the overall pressure drop (friction factor) for the reactors UA200.08 and UA63.03 (homemade laboratory filter-press reactors previously studied[35]) with other electrochemical filter-press reactors such as FM01-LC from ICI. The measurements include the pressure drop associated with manifolds. The total pressure drop across the electrolyzers is relatively high because of the restriction to the flow imposed by the design of the manifolds. Thus, for the majority of the promoters, the increase in the pressure drop across the internal channel was undetectable compared to the total pressure drop without promoters. In Figure 4, we have not plotted the Poiseuille flow result which is applicable to open channels in laminar flow at *Re* below 2300[37] because the results for our practical reactors are located far away from this line, showing the natural nonfully laminar of the flow inside the reactors. However, for *Re* lower than 1000, the friction factor, $f = \Delta P d_e/2\rho L v^2$, begins to increase as *Re* decreases, suggesting that this value can be Re_{crit} and the flow dynamics within the cell could enter the laminar−turbulent transition pattern. This number of $Re = 1000$ is an approximate value, calculated by the union of the two straight lines representing the extreme cases for very high and very low *Re* (in agreement with ref 38). This behavior is in agreement with that found in the literature.[39]

3.1.2. RTD. The experimental outlet conductivity registered as a function of time allows the RTD to be established. The study of the tracer curves is usually carried out using flow models by means of modeling the fluid flow in the whole electrolyzer.

3.1.2.1. Models for the Representation of the Electrochemical Reactor. The two common theoretical models used to describe flow characteristics, plug flow and perfect mixing, are not suitable for characterizing the hydrodynamic behavior inside the electrochemical filter-press cell. The real reactors normally present dispersion phenomena, dead or stagnant zones, bypass flows, exchanges between them, recirculation zones, etc. The present literature on this subject uses simple dispersion models, particularly the axially dispersed plug-flow model, to obtain a representation of the reactor. This model presents two parameters, namely, the Peclet number and the mean residence time and is formulated by the equation

$$\frac{\partial C}{\partial \theta} = -\frac{\partial C}{\partial Z} + \frac{1}{Pe}\frac{\partial^2 C}{\partial Z^2} \qquad (1)$$

where *C* is the normalized concentration of the measured property, $Z = z/L$, with *L* being the total length of the reactor in the flow direction where the only observable dispersion takes place, $\theta = t/\tau$, with τ being the average residence time, and *Pe* is the Peclet number ($=vL/D_{ax}$).

The application of this model presents many problems when the tailing phenomena appear in the tracer curves.[32] These tailing phenomena have been observed in reactors which contain fast and stagnant phases or fluid areas with long residence times, and special models have been set up to describe them.[40−43] Van Swaaij calls such models "combined models", because they consist of a combination of plug-flow zones, ideally mixed zones, bypass flow elements, and dead zones. Combined models may have to be taken into consideration if great accuracy is required in the modeling of the state of mixing. However, drawbacks such as the loss of physical meaning are normally highlighted in this type of approach.

In the present work, the experimental RTD curves for the UA200.08 electrochemical reactor cannot be modeled by the pure axially dispersed plug-flow model because the RTD responses present the tailing phenomena. A combined model has been used, plug flow with axial dispersion and flow exchange with stagnant and/or dead zones, presented when the laboratory filter-press reactor[35] was studied. This model is an adaptation of a more complex model used for three-dimensional

Table 2. Results of the RTD Modeling for the Empty Configuration and for the Configuration with Turbulence Promoters

	empty			promoter A			promoter B			promoter C_s			promoter C_l			promoter D		
Re	Φ_β	*Pe*	N_α	Φ_β	*Pe*	N_α	Φ_β	*Pe*	N_α	Φ_β	*Pe*	N_α	Φ_β	*Pe*	N_α	Φ_β	*Pe*	N_α
75	0.61	13	0.71															
106				0.67	295	1.83	0.66	307	1.69	0.66	281	1.90	0.61	828	1.70	0.62	317	1.59
161				0.70	470	1.41	0.66	561	1.58	0.65	465	1.56	0.63	892	1.68	0.70	289	1.67
227	0.58	40	0.88															
243				0.71	264	1.36	0.70	485	1.26	0.70	246	1.29	0.66	285	1.31	0.71	424	1.08
298				0.72	488	1.33	0.71	127	1.15							0.71	241	1.32
346	0.58	13	0.83															
499	0.50	27	1.03															

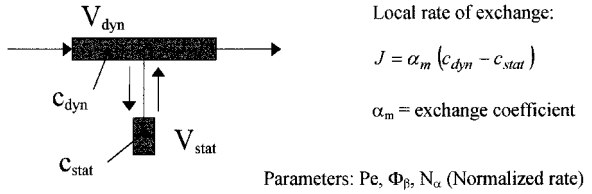

Figure 5. Sketch of the model for the flow characterization.

electrodes[36] and is based on a previous work.[41] A sketch of the model is shown in Figure 5.

The flow model for the reactor is a dispersed plug flow with stagnant areas; the electrolyte in these stagnant areas is slowly refreshed by the freely flowing electrolyte that can be considered in axially dispersed plug flow. The electrolyte holdup in this zone, β_{tot} = m^3 of liquid/m^3 of column, is divided into a dynamic holdup, β_{dyn}, and a static or stagnant holdup, β_{stat}. The local rate of exchange between the dynamic and static holdup is assumed to be proportional to the concentration difference in the dynamic and static phases and can be characterized by an exchange coefficient, α_m (s^{-1}), defined by

$$J = (\text{number of moles exchanged})/(\text{m}^3 \text{ of liquid}\cdot\text{s}) = \alpha_m(c_{dyn} - c_{stat}) \quad (2)$$

where c_{dyn} and c_{stat} are the concentrations in the dynamic and static phases, respectively. α_m can be considered as the product of a mass-transfer coefficient and the specific interfacial area between the flowing and the stagnant zones, $k_L a$.

The model equations can be found from a mass balance for the dynamic (dyn) and the static (stat) phases over a thin slice perpendicular to the direction of the flow, whereas the density and other variables are assumed to be constant over the length coordinates:[40]

$$\Phi_\beta \frac{\partial C_{dyn}}{\partial \theta} = \frac{1}{Pe}\frac{\partial^2 C_{dyn}}{\partial Z^2} - \frac{\partial C_{dyn}}{\partial Z} - N_\alpha(C_{dyn} - C_{stat}) \quad (3)$$

$$(1 - \Phi_\beta)\frac{\partial C_{stat}}{\partial \theta} = -N_\alpha(C_{stat} - C_{dyn}) \quad (4)$$

where $Z = z/L$, with L being the total length of the reactor, $\Phi_\beta = \beta_{dyn}/\beta_{tot}$, $N_\alpha = \alpha_m L/\Phi_\beta v_l$, $Pe = v_l L/D_{ax}$, $\theta = t/\tau$, with $\tau = L/\Phi_\beta v_l$, $C_{stat} = c_{stat}/c$, $C_{dyn} = c_{dyn}/c$, S = cross-sectional area of volume V_{dyn} (m^2), v_l = velocity in the dynamic phase of volume $V_{dyn} = Q_l/S\beta_{dyn}$, Q_l = electrolyte flow through volume V_{dyn} ($m^3\ s^{-1}$), and D_{ax} = dispersion coefficient in the dynamic phase ($m^2\ s^{-1}$).

In this way, N_α is the number of mass-transfer units for the mass exchange between the dynamic and static phases and *Pe* is the Peclet number for the dynamic phase.

The parameters of the model are only three (*Pe*, Φ_β, and N_α), and all of them have a clear physical meaning, as stated above.

Figure 6 shows the experimental recording for the empty reactor and for the reactor with the promoters, for the runs performed at *Re* = 106 and 298. A great difference exists between the empty reactor and the reactor with promoters. The empty reactor presents a typical curve corresponding to the existence of a dead zone, for all of the flow rates studied. Furthermore, at low flow rates, the recording presents some noise that could give an idea of the complexity of the hydrodynamics in the system. The incorporation of the promoters considerably modifies the experimental curve, eliminating the noise, decreasing the tail of the curve, and closing the maximum of the curve to the point $t/\tau = 1$, especially at high *Re*. Figure 7 shows the overstrike of the experimental and simulated curves (reactor with promoter C_s) for (I) a model with no exchange between the dead and main zones of the reactor and (II) a model that considers this exchange. Model I does not assume a good approximation of the system, because it is not able to simulate the tailing phenomena. Furthermore, model I gives dead volumes close to zero, a fact that is not deduced from the experimental form of the curves.

The optimization of the curves with the model was carried out using very different initial sets of parameters, in the entire range of possible values and for values of $t/\tau < 3$. In almost all of the cases, all of the initial sets lead the optimization to the same minimum. The objective function was defined as

$$\text{O.F.} = \sum_i (x_i^{calc} - x_i^{exp})^2 \quad (x_i = \text{point of the RTD curve}) \quad (5)$$

The value of the O.F. was around 10^{-3} for the majority of the curves, going from 10^{-4} for the curves corresponding to low values of *Re* to 10^{-2} for the curves of high *Re*. The variation coefficient can also be defined, to quantify the quality of the fitting:

$$\text{V.C. (\%)} = \frac{\sqrt{\dfrac{\text{O.F.}}{N - P}}}{\bar{x}_{exp}} \quad (6)$$

where N is the total number of points, P is the number of parameters to be fitted, and $\bar{x}_{exp}$ is the mean value of the experimental data used in the O.F. (eq 5). The values of this V.C. are between 1 and 3% for the best modeling for all of the curves measured.

During the optimization process, a high dependence on the parameter Φ_β was observed, in such a way that only if this parameter presented the adequate value, was the O.F. acceptable. Furthermore, this is the first

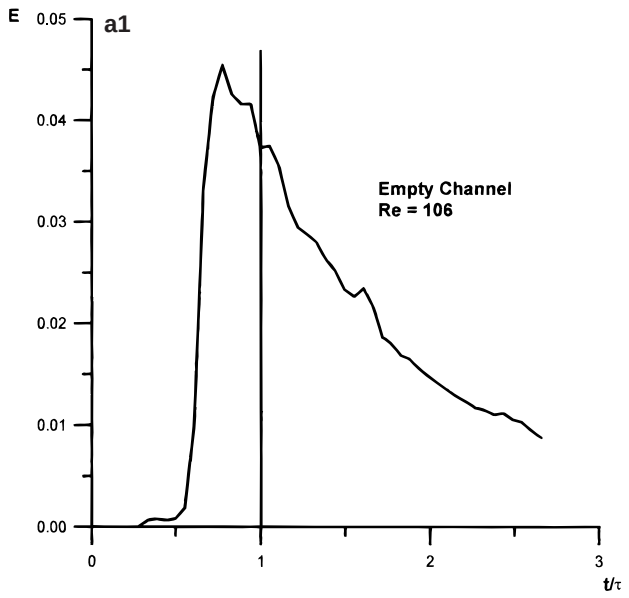
a1
E
0.05
0.04
0.03
0.02
0.01
0.00
0
1
2
3
t/τ
Empty Channel
Re = 106

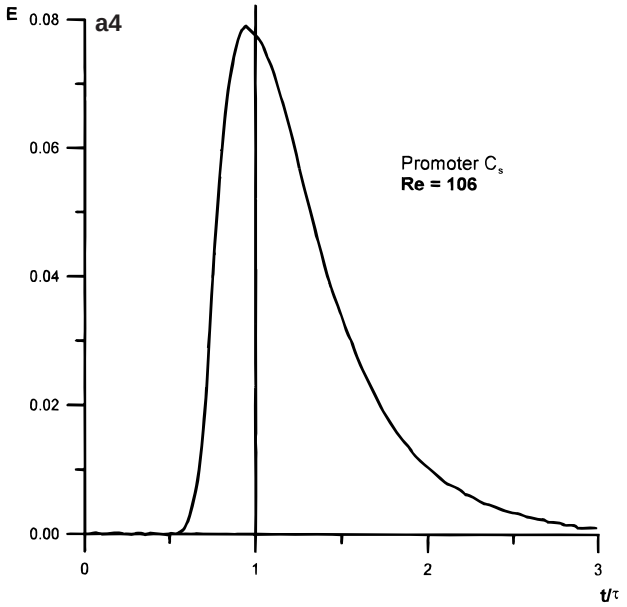
a4
E
0.08
0.06
0.04
0.02
0.00
0
1
2
3
t/τ
Promoter C$_s$
Re = 106

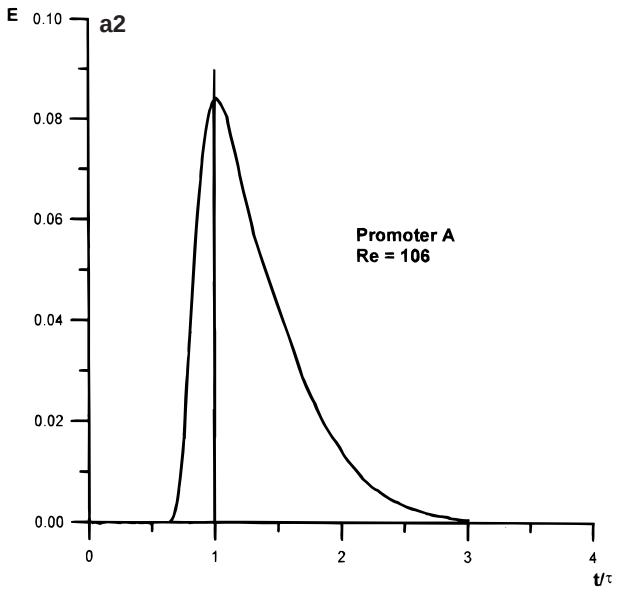
a2
E
0.10
0.08
0.06
0.04
0.02
0.00
0
1
2
3
4
t/τ
Promoter A
Re = 106

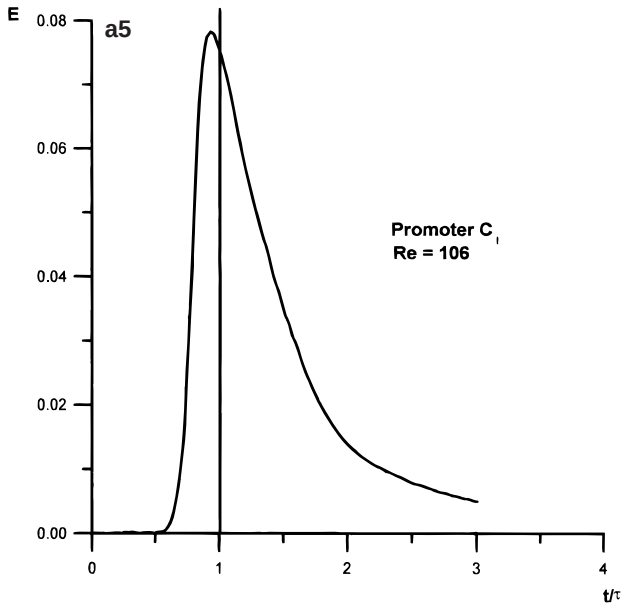
a5
E
0.08
0.06
0.04
0.02
0.00
0
1
2
3
4
t/τ
Promoter C$_t$
Re = 106

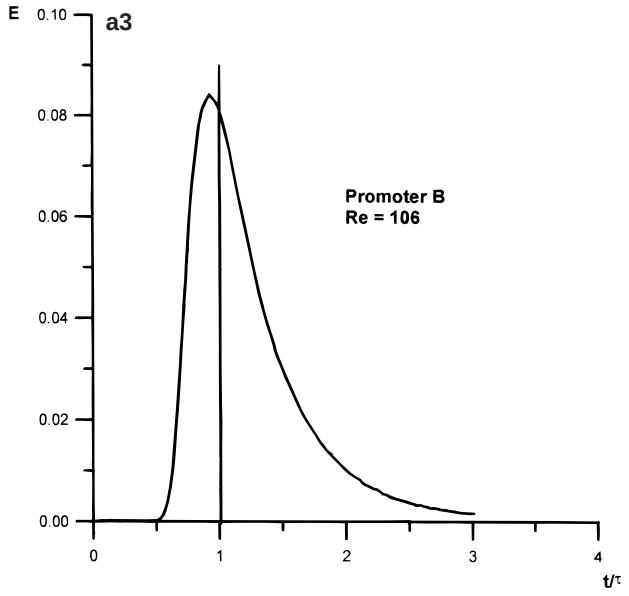
a3
E
0.10
0.08
0.06
0.04
0.02
0.00
0
1
2
3
4
t/τ
Promoter B
Re = 106

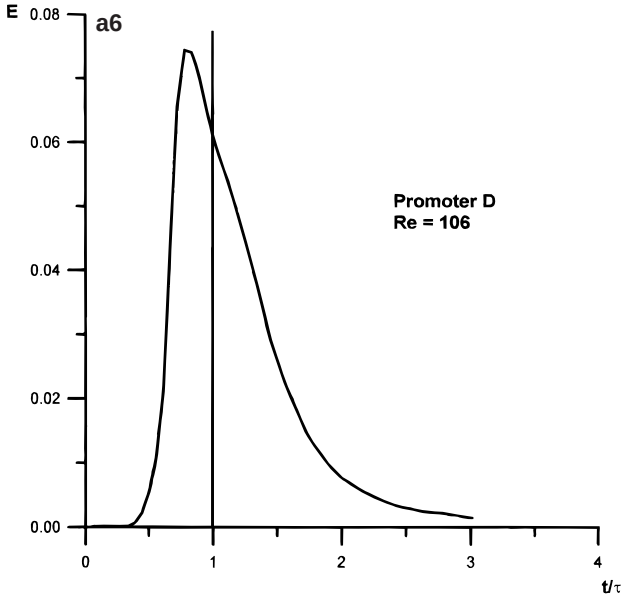
a6
E
0.08
0.06
0.04
0.02
0.00
0
1
2
3
4
t/τ
Promoter D
Re = 106

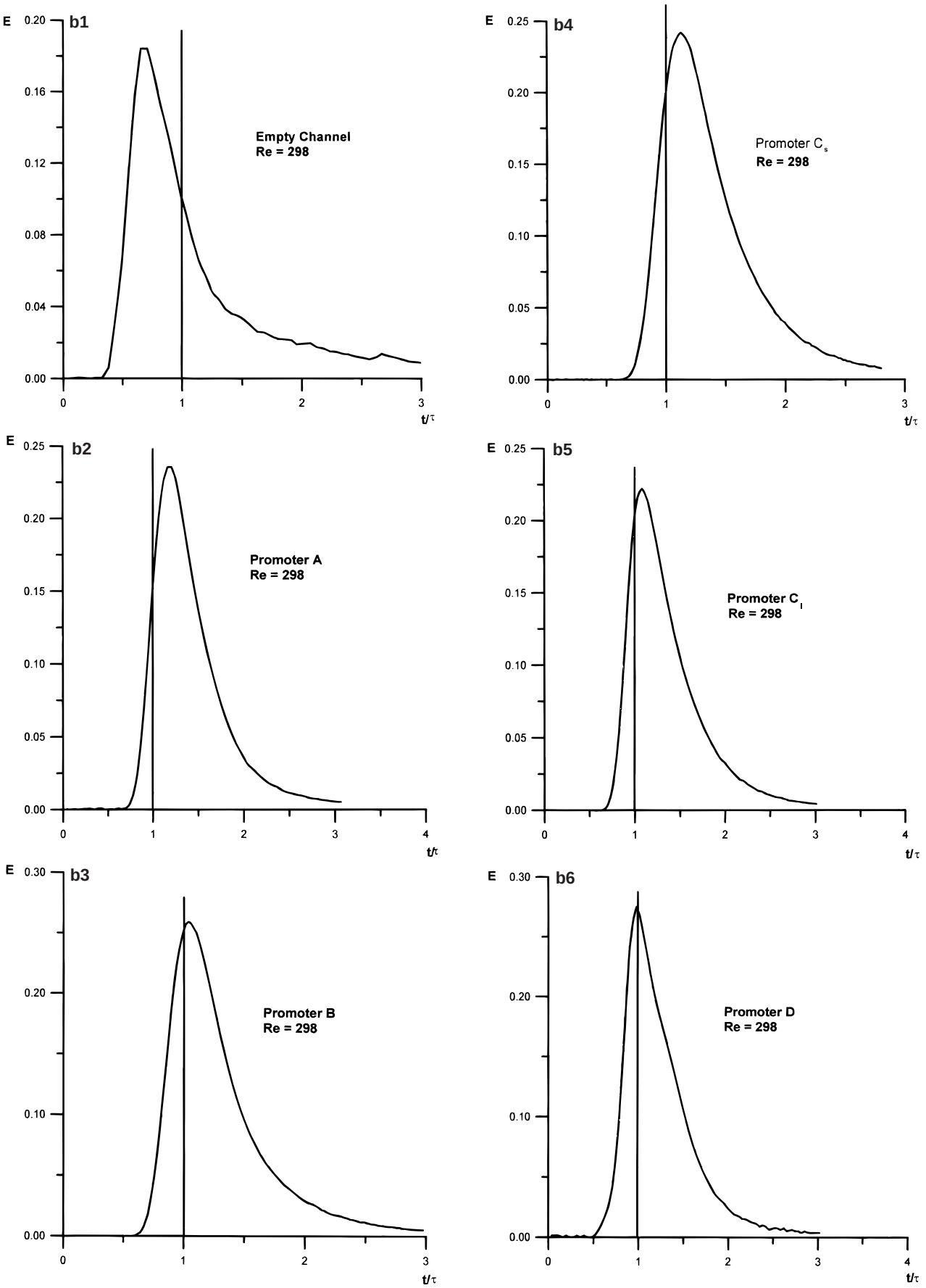

Figure 6. Experimental RTD obtained for the empty configuration and with different promoters: (a1) $Re = 106$, empty channel; (a2) $Re = 106$, promoter A; (a3) $Re = 106$, promoter B; (a4) $Re = 106$, promoter C_s; (a5) $Re = 106$, promoter C_l; (a6) $Re = 106$, promoter D; (b1) $Re = 298$, empty channel; (b2) $Re = 298$, promoter A; (b3) $Re = 298$, promoter B; (b4) $Re = 298$, promoter C_s; (b5) $Re = 298$, promoter C_l; (b6) $Re = 298$, promoter D (details in the figure).

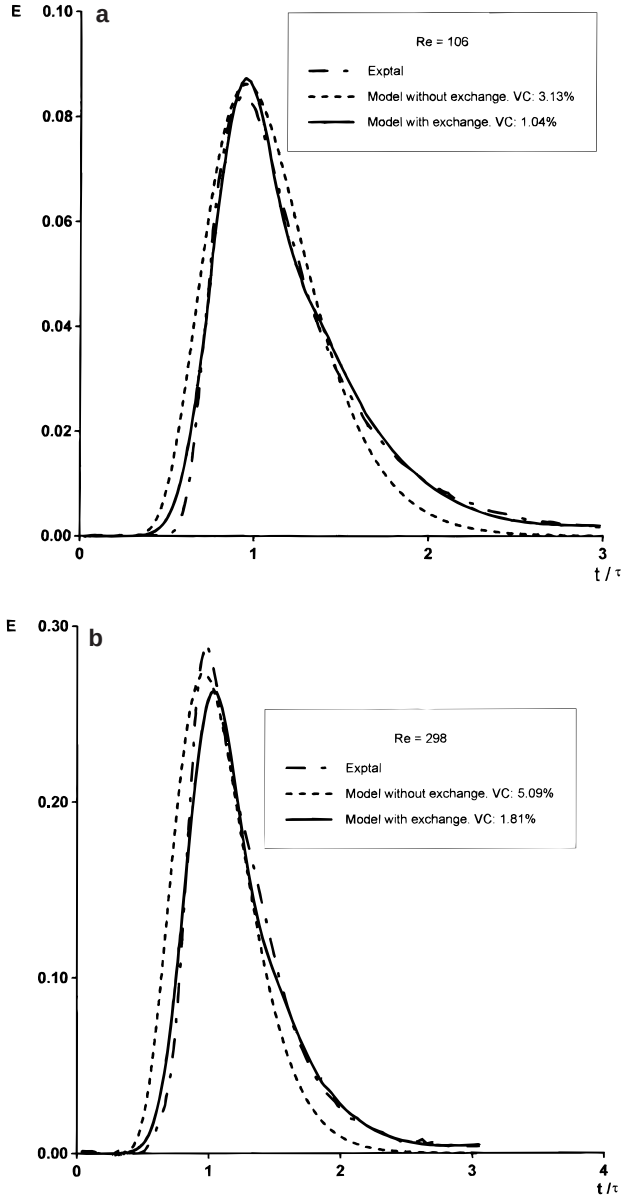

Figure 7. Experimental and simulated curves obtained with two models studied: (a) $Re = 106$, (b) $Re = 298$ (details in the figure). V.C. is the variation coefficient.

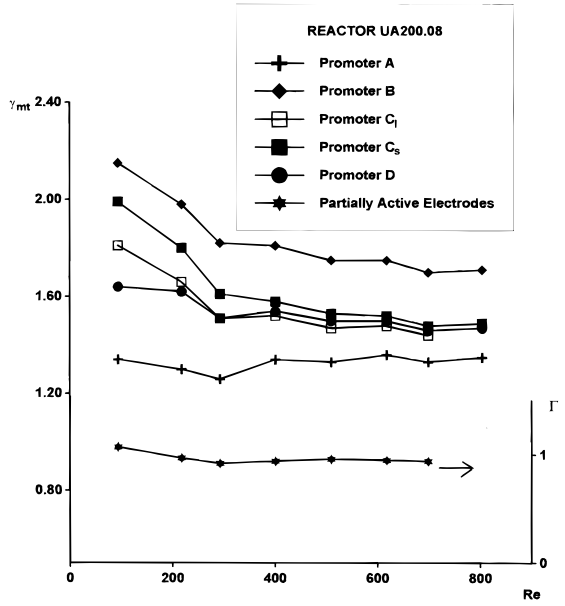

Figure 8. Mass transport enhancement and correcting factors in reactor UA200.08.

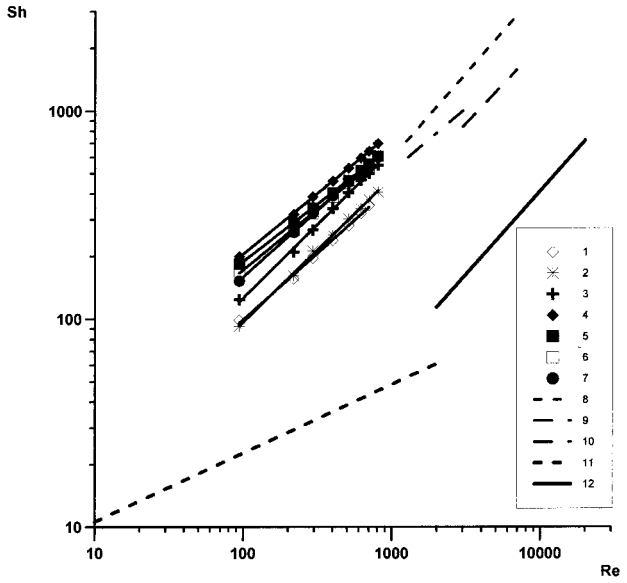

Figure 9. Dimensionless group mass transport correlations for the reactor UA200.08 (promoted and unpromoted configuration) showing a comparison with other studies in the literature: 1. partially active electrode (empty configuration), eq 11; (2) free electrode (empty configuration), eq 10; (3) promoter A, eq 12; (4) promoter B, eq 13; (5) promoter C_s, eq 15; (6) promoter C_l, eq 14; (7) promoter D, eq 16; (8) eq 7 from Table 3 (ref 26); (9) eq 8 from Table 3 (ref 26); (10) eq 9 from Table 3 (ref 47); (11) laminar flow eq 17 from Table 3 (ref 21); (12) turbulent flow eq 18 from Table 3 (ref 21).

parameter that the optimization process finds and does not vary any more.

Table 2 presents the results of the optimization. Despite the difficulty in the simulation of the curves for the empty configuration, especially at low values of *Re* due to the noise, a great difference exists between the parameters for the empty and promoted reactors. The model provides lower values of N_α, Φ_β, and *Pe* for the empty reactor. In the configurations with turbulence promoters, an increase of Φ_β and a decrease of N_α when *Re* increases can be observed. An opposite tendency is followed in the empty configuration.

3.2. Mass Transport Study. Figure 8 summarizes the results obtained by means of the mass transport study. It shows the correcting factor, Γ, defined in the Nomenclature section, and the mass transport enhancement factor, γ_{mt}, defined by Walsh and Reade.[44] The first factor analyzes the influence on the mass transport of the streams flowing from the electrolyte in the compartment flow distributors into the reaction zone. This parameter is especially important in practical reactors without deliberate calming lengths, to measure the influence of this entrance effect on mass transport behavior at relatively low *Re*. The values obtained are near 0.93. This means that the inlet/outlet effect of these reactors is less obvious than laboratory filter-press reactors[35] with descending values from 0.88 until 0.74 as *Re* increases. As the electrode length is increased, the mass transport enhancement at the inlet/outlet zones presents less influence in the space-averaged mass transport.

The behavior of the mass transport enhancement factor, γ_{mt}, presents a general trend toward lower values

Table 3. Mass Transport Correlations for the Reactor UA200.08 and Other Pilot-Plant Reactors Found in the Literature

		$Sh = a'Re^bSc^c$				
reactor	equation	a'	b	c	conditions	reference
unnamed					area = 225 cm^2, $L_e = 15.4 \times 10^{-2}$, $\gamma = 0.1$	
empty	7	0.19	0.812	0.33	$1250 < Re < 6900$	26
baffled	8	0.18	0.75	0.33	$Re > 3000$	26
baffled	9	0.46	0.66	0.33	$3000 < Re < 15000$	47
UA200.08					area = 216 cm^2, $L_e = 1.28 \times 10^{-2}$, $\gamma = 0.04$	
empty						
free	10	0.35	0.70	0.33	$94 < Re < 804$	present study
part. activ.	11	0.15	0.64	0.33	$94 < Re < 804$	present study
promoted						
type A	12	0.43	0.71	0.33	$94 < Re < 804$	present study
type B	13	1.24	0.58	0.33	$94 < Re < 804$	present study
type C_l	14	1.03	0.59	0.33	$94 < Re < 804$	present study
type C_s	15	1.31	0.55	0.33	$94 < Re < 804$	present study
type D	16	0.75	0.64	0.33	$94 < Re < 804$	present study

Theory

		$Sh = aRe^bSc^cL_e^d$					
		a	b	c	d		
laminar	17	1.85	0.33	0.33	0.33	$Re < 2000$	21
turbulent	18	0.023	0.8	0.33		$Re > 2000$	21

at higher *Re*, lying between 2.20 and 1.30. Furthermore, we have used the promoter *C* in order to point out the promoter orientation effects, and the results are in agreement with other authors.[45,46]

The mass transport coefficients were put into dimensionless form by means of the Sherwood number definition, and the dimensionless mass transport correlation was obtained in order to compare this reactor with other similar reactors found in the literature (Table 3). In Figure 9 the mass transport correlations from Table 3 have been plotted with the theoretical equations for fully developed laminar flow and fully developed turbulent flow.[21] It can be seen that the slope of the correlations is higher than the theoretical expressions in the laminar *Re* region and is very similar to those shown by the theoretical turbulent expression. This behavior has also been observed by several authors[17,29,48,49] for a wide group of commercial and homemade reactors. The explanation for this behavior is that the inexistence of calming zones in the reactor involves the direct injection of the electrolyte into the compartment. This fact, together with the limited length of the compartment in the flow direction, avoids the fully developed laminar flow pattern. However, this situation could not only be attributed to the direct injection effect, because the mass transport correlation for the partially active electrodes does not present a significant change in the slope, 0.64, higher than the theoretical 0.33. In addition, the behavior of the friction factor at this range of *Re* numbers supports this representation. On the other hand, it should be noted that the mass transport correlation for the partially active electrode presents a lower average rate of mass transport, lower values of a' and b.

The presence of the turbulence promoters involves a decrease in the exponent of *Re* and an increase of the parameter a' with respect to the empty configuration. This behavior has been widely reported in the literature,[17,27−29,37,50] and the explanations given are related to electrolyte channeling phenomena.

4. Discussion

The modeling of the RTD responses provides interesting information in order to analyze the influence of the promoters. The low values of the parameter Φ_β and *Pe* for the empty configuration, in contrast with the configuration with turbulence promoters, permit a representation of the reactor to be imagined consisting of a great fraction of the reactor volume with low dynamic zones, and possibly recirculations. This complex representation agrees with the noise in the experimental curves. Furthermore, the ascending trend for *Pe* with *Re* supports this representation. This situation is in agreement with other findings reported by other authors. Investigations of changes in flow at the entry of electrochemical flow cells[51−54] have been reported in the literature. In these works, a relationship between mass transport distribution and the recirculation zone hydrodynamics has been established by determining the local limiting current: the flow suddenly expands into a cell, and a region of recirculating flow occurs with high mass transport. Near the corners of the rectangular cells, secondary flows are known to occur in both laminar and turbulent conditions with high mass transport also. At a short distance into the cell, the flow begins to develop in the normal way. For example, for a square cross-sectional cell, a notable feature is the fact that, in the recirculation zone, the mass transport in the center is higher than the mass transport at the corner. In the far downstream region, this pattern is reversed and the corner mass transport is the highest. More recently, hydrodynamic behavior studies by means of local mass transport analysis in parallel-plate electrochemical reactors with baffled and unbaffled[35] and promoted configurations[17,55] have been reported in the literature. In these works, a global swirling motion in the cell, driven by the inlet jets with relatively inactive zones, was described for empty configurations, and a more uniform pattern imposed by the turbulence promoters is obtained. A similar situation can be deduced with our results from the RTD modeling in the promoted configuration: higher Φ_β and a strong enhancement in the *Pe* number is obtained. The presence of the promoter obstructs the development of the relatively stagnant zones (higher Φ_β) and can produce a great number of smaller channels, which produces a decrease of the dead and stagnant zones. In this way, the mass transport to the electrode is less dependent on the flow rate (minor

Table 4. Values of $N_\alpha\Phi_\beta$ for the Different Turbulence Promoters and Different Reynolds Numbers

Re	empty	promoter A	promoter B	promoter C_s	promoter C_l	promoter D
75	0.43					
106		1.23	1.12	1.25	1.04	0.99
161		0.99	1.13	1.01	1.06	
227	0.49					
243		0.96	0.88	0.9	0.86	0.76
298		0.96	0.82			0.93
346	0.49					
499	0.52					

value of the exponent of *Re* in the mass transport correlation) and does depend more on the promoter characteristics (higher value of *a*).

The more detailed study of the difference between turbulence promoters presents more difficulties. These difficulties have also been presented previously in the literature.[46] The formation of eddies occurs because the inclusion of promoters is the reason for the increment of the mass transport to the electrode. The mechanism, following the RTD model proposed above, is a combination of the decrease of the volume of the stagnant zones (higher value of Φ_β) and the increase of the mass transfer between the dynamic and static zones, which are still close to the walls of the reactor. The increase of the Φ_β value is particularly important in the zones that are close to the electrode. In this respect, it is logical to assume that the introduction of turbulence promoters greatly diminishes the edge effects, particularly in the lab- and bench-scale reactors, from the hydrodynamical point of view.

The mass transport enhancement coefficient is the more adequate parameter to carry out the comparative study with the limiting current technique. The transformation of these experimental data using the mass transport correlation allows the values of the coefficients a' and b to be obtained.

To relate the results obtained by means of the mass transport study with the results from the hydrodynamic study, a comparison between the parameters a' and b and the optimization parameters *Pe* and Φ_β was carried out. The promoters A and D, with minor diagonal distances, present velocity exponents and Φ_β normally higher than those of the other promoters. To classify the turbulence promoters, in the previous paper[35] a turbulence factor, $N_\alpha\Phi_\beta$, was proposed. For a constant value of Φ_B, an increase in N_α, the rate of exchange, will produce a higher degree of turbulence. In the same way, for a constant value of N_α, an increase in Φ_β will produce a higher part of the reactor acting as plug flow, so the turbulence is also promoted. For this reason the product $N_\alpha\Phi_\beta$ has been considered as a turbulence factor measuring the turbulence promoter effectiveness. Table 4 shows the results obtained. The parameter $N_\alpha\Phi_\beta$ for the promoters shows a descending trend in the same way as the mass transport enhancement coefficient, but the promoter classification is not direct. Only the behavior of the promoter A is opposite to the behavior predicted using the mass transport study:

mass transport: $B > C_s > C_l > D > A$

RTD modeling: $A > B \approx C_s > C_l > D$

The anomalous behavior of promoter A could be associated with its nonuniform fiber distribution, as can be appreciated in its "double graph" (Figure 2), which permits a more compact packing. This phenomenon produces a greater "blinding" of the walls, favoring the canalization of the electrolyte in the flow direction.

5. Conclusions

The modeling of the RTD response and the information obtained from the turbulence factor is presented as an alternative nonelectrochemical method for the characterization of reactors.

Furthermore, this technique is particularly useful for reactors of great dimensions, where the utilization of the electrochemical techniques (availability of a high-power potentiostat, incorporation of reference electrodes in the commercial compartments, etc.) is not always direct. At the moment the validation of this method in the full pilot-plant scale (electrode area 1000 cm^2) and industrial scale (3300 cm^2) is in progress.

In this way, a representation of the reactor by means of models simulating the experimental RTD responses could be helpful in the exploration of local mass transport distributions. Combined models, which permit hydrodynamic phenomena to be introduced, are especially useful.

Acknowledgment

J.G.-G. thanks "Consellería de Cultura, Educación y Ciencia, Generalidad Valenciana" for his doctoral grant. The authors also thank the "D.G.I.C.Y.T. (Project QUI97-1086)" and "Generalidad Valenciana" (Project GV-2231-94) for their financial support.

Nomenclature

a, a' = coefficients of the mass transport correlation or specific interfacial area between the flowing and stagnant zones, m^2/m^3
B = breadth of the compartment (perpendicular to the direction of flow), m
b = Reynolds exponent in the mass transport correlation
c = concentration (or Schmidt exponent in the mass transport correlation), mol/m^3
c_{dyn} = concentration in the main flow, mol/m^3
c_{stat} = concentration in the dead zones, mol/m^3
C = normalized concentration
d = exponent of the dimensionless length group in the mass transport correlation
d_e = equivalent (hydraulic) diameter of the compartment ($=2Bs/(B + s)$), m
D = diffusion coefficient, m^2/s
D_{ax} = dispersion coefficient in the axial direction, m^2/s
E = residence time distribution (RTD)
f = friction factor ($=\Delta P d_e/2\rho L v^2$)
J = rate of exchange between the stagnant and main flow, mol/m^3 s
k_L = mass-transfer coefficient between the flowing and stagnant zones, m/s
k_m = mass transport coefficient, m/s
L = length of the compartment in the direction of flow, m

L_e = dimensionless length group ($=d_e/L$)
N_α = normalized rate of exchange between dispersed plug-flow and dead zones
$N_\alpha\Phi_\beta$ = turbulence factor
ΔP = pressure drop, Pa
Pe = Peclet number ($=vL/D_{ax}$)
Re = Reynolds number ($=vd_e/\nu$)
Re_{crit} = theoretical value of Re for change from laminar to turbulent flow
Q_v = volumetric flow rate, m^3/s
S = cross-sectional of volume V_{dyn}, m^2
Sc = Schmidt number ($=\nu/D$)
Sh = Sherwood number ($=k_m d_e/D$)
s = thickness of the compartment, m
t = time, s
V.C. = variation coefficient
V_{dyn} = volume of the dynamic region of the reactor, m^3
V_{stat} = volume of the stagnant region of the reactor, m^3
v = mean linear velocity, m/s
z = coordinate in the direction of flow, m
Z = normalizated coordinate in the direction of flow

Greek Letters

α_m = exchange coefficient between main flow and stagnant zones, s^{-1}
β_{tot} = electrolyte holdup ($=m^3$ of liquid/m^3 of column)
β_{dyn} = dynamic holdup
β_{stat} = stagnant holdup
Φ_β = fraction between dispersed plug-flow and total volume
γ = aspect ratio of the compartment ($=s/B$)
γ_{mt} = enhancement factor (k_m(with promoter)/k_m(without promoter))
Γ = correcting factor (k_m(partially blocked electrode)/k_m(free electrode))
ν = kinematic viscosity, m^2/s
θ = dimensionless time.
ρ = density, kg/m^3
τ = mean residence time for the compartment, ($=V_t/Q_v$) where V_t is the volume offered to the flow, taking into account the presence of turbulence promoters inside the reactor, s

Literature Cited

(1) Walsh, F. C.; Reade, G. Design and Performance of Electrochemical Reactors for Efficient Synthesis and Environmental Treatment. Part 2. Typical Reactors and their Performance. *Analyst* **1994**, *119*, 797.

(2) Couper, A. M.; Pletcher, D.; Walsh, F. C. Electrode materials for electrosynthesis. *Chem. Rev.* **1990**, *90*, 837.

(3) González-García, J.; García-García, V.; Montiel, V.; Aldaz, A. Industrial Synthesis of Cisteine derivatives. Presented at the European Research conferences "Organic Electrochemistry: Moving Towards Clean and Selective Synthesis", Agelonde, France, April 15−19, 1998.

(4) Sánchez-Cano, G.; Montiel, V.; García, V.; Aldaz, A.; Elías, E. From voltammetry to industrial plant: Electrochemical synthesis of DL-Homocysteine from DL-Homocystine—an example of scale-up. In *Electrochemical Engineering and Energy*; Lapicque, F., et al., Eds.; Plenum Press: New York, 1995.

(5) Sánchez-Cano, G.; Montiel, V.; Aldaz, A. Synthesis of L-cysteic acid by indirect electrooxidation and an example of paired synthesis: L-cysteic and L-cysteine form L-cystine. *Tetrahedron* **1991**, *47*, 877.

(6) Pletcher, D. *A First Course in Electrode Processes*; The Electrochemical Consultancy: Romsey, 1991; p 201.

(7) Talbot, J. B.; Fritts, S. D. Report of the Electrolytic Industries for the Year 1991. *J. Electrochem. Soc.* **1992**, *139*, 2981.

(8) Bergner, D. Membrane electrolyzers for chlor−alkali Industry. *DECHEMA Monogr.* **1991**, *123*, 113.

(9) Marshall, R. J.; Walsh, F. C. A review of some recent electrolytic cell designs. *Surf. Technol.* **1985**, *24*, 45.

(10) Walsh, F. C.; Robinson, D. Electrochemical filter-press reactors. *Interface* **1998**, *7* (2), 40.

(11) White, R. E. *Electrochemical Cell Design*; Plenum Press: New York, 1984.

(12) Heitz, E.; Kreysa, G. *Principles of Electrochemical Engineering*; VCH: Weinheim, Germany, 1986; p 53.

(13) Genders, J. D.; Pletcher, D. *Electrosynthesis: from laboratory to Pilot to Production*; The Electrochemical Consultancy: Romsey, 1991.

(14) Scott, K. The effect of electrode ohmic losses and the role of the electrical connection in bipolar connected parallel plate electrodes. *Electrochim. Acta* **1983**, *28*, 133.

(15) Bonvin, G.; Comninellis, Ch. Scale-up of a bipolar electrode stack dimensionless numbers for current bypass estimation. *J. Appl. Electrochem.* **1994**, *24*, 469.

(16) Ponce de León, C.; Pletcher, D. The removal of Pb(II) from aqueous solutions using a reticulated vitreous carbon cathode cell—the influence of the electrolyte medium. *Electrochim. Acta* **1996**, *41*, 533.

(17) Taama, W. M.; Plimley, R. E.; Scott, K. Mass transfer rates in a DEM electrochemical cell. *Electrochim. Acta* **1996**, *41*, 543.

(18) Janssen, L. J. J.; Visser, G. J. Behaviour of a tall vertical gas-evolving cell. Part I: Distribution of void fraction and of ohmic resistance. *J. Appl. Electrochem.* **1991**, *21*, 386.

(19) Bisang, J. M. Effect of mass transfer on the current distribution in monopolar and bipolar electrochemical reactors with a gas-evolving electrode. *J. Appl. Electrochem.* **1993**, *23*, 966.

(20) Walsh, F. C. *A first course in electrochemical engineering*; The Electrochemical Consultancy: Romsey, 1993; p 266.

(21) Pickett, D. J. *Electrochemical Reactor Design*; Elsevier: Amsterdam, The Netherlands, 1979.

(22) Coeuret, F.; Storck, A. *Elements de Génie Electrochimique*; Tec-Doc Lavoisier: Paris, 1984.

(23) Pletcher, D.; Walsh, F. C. *Industrial Electrochemistry*; Chapman and Hall: London, 1990.

(24) Nguyen, T. V.; Walton, C. W.; White, R. E.; Van Zee, J. Parallel-Plate Electrochemical Reactor Model. A method for determining the time-dependent behaviour and the effects of axial diffusion and axial migration. *J. Electrochem. Soc.* **1986**, *133*, 81.

(25) Wragg, A. A.; Leontaritis, A. A. Local mass transfer and current distribution in baffled and unbaffled parallel plate electrochemical reactors. *Chem. Eng. J.* **1997**, *66*, 1.

(26) Wragg, A. A.; Leontaritis, A. A. Mass transfer measurements in a parallel cell using the limiting current technique. *DECHEMA Monogr.* **1991**, *123*, 345.

(27) Müler, V.; Rousar, I. Mass transfer coefficient and pressure losses for membrane cell with spacers. *DECHEMA Monogr.* **1991**, *123*, 331.

(28) Letord-Quémere, M. M.; Coeuret, F.; Legrand, J. Mass transfer at the wall of a thin channel containing an expanded turbulence promoting structure. *J. Electrochem. Soc.* **1988**, *135*, 3063.

(29) Carlsson, L.; Sandegren, B.; Simonsson, D.; Rihovsky, M. Design and performance of a modular, multi-purpose electrochemical reactor. *J. Electrochem. Soc.* **1983**, *130*, 342.

(30) Bengoa, C.; Montillet, A.; Legentilhomme, P.; Legrand, J. Flow visualization and modelling of a filter-press type electrochemical reactor. *J. Appl. Electrochem.* **1997**, *27*, 1313.

(31) Montillet, A.; Legrand, J.; Commiti, J.; Letord, M. M.; Jud, J. M. Use of metallic foams in electrochemical reactors of filter-press type: mass transfer and flow visualization. *Electrochemical Engineering and Energy*; Lapicque, F., Eds.; et al., Plenum Press: New York, 1994.

(32) Trinidad, P.; Walsh, F. C. Hydrodynamic behaviour of the FM01-LC reactor. *Electrochim. Acta* **1996**, *41*, 493.

(33) Montillet, A.; Commiti, J.; Legrand, J. Application of metallic foams in electrochemical reactors of filter-press type. Part I: Flow characterization. *J. Appl. Electrochem.* **1993**, *23*, 1045.

(34) Carpenter, N. G.; Roberts, E. P. L. Mass transport and residence time characteristics of an oscillatory flow electrochemical reactor. *Inst. Chem. Eng. Symp. Ser.* **1999**, *145*, 309.

(35) González-García, J.; Conesa, J. A.; Iniesta, J.; García-García, V.; Montiel, V.; Aldaz, A. *Inst. Chem. Eng. Symp. Ser.* **1999**, *145*, 51.

(36) González-García, J.; Montiel, V.; Aldaz, A.; Conesa, J. A.; Pérez, J. R.; Codina, G. Hydrodynamic Behavior of a Filter-Press Electrochemical Reactor with Carbon Felt as a Three-Dimensional Electrode. *Ind. Eng. Chem. Res.* **1998**, *37*, 4501.

(37) Brown, C. J.; Pletcher, D.; Walsh, F. C.; Hammond, J. K.; Robinson, D. Studies of space-averaged mass transport in FM01-LC laboratory electrolyser. *J. Appl. Electrochem.* **1993**, *23*, 38.

(38) Holland, F. A. *Fluid flow for Chemical Engineers*; Edward Arnold: London, 1973; p 21.

(39) Roberts, R.; Ouellette, R. P.; Cheremisinoff, P. N. *Industrial Applications of Electroorganic Synthesis*; Ann Arbor Science: Ann Arbor, MI, 1983; p 43.

(40) Westerterp, K. R.; van Swaaij, W. P. M.; Beenackers, A. A. C. M. *Chemical Reactor Design and Operation*; John Wiley & Sons: Chichester, U.K., 1993.

(41) Villermaux, J.; van Swaaij, W. P. M. Modèle représentatif de la distribution des temps de séjour dans un réacteur semi-infini à dispersion axiale avec zones stagnantes. Application à l'écoulement ruisselant dans des colonnes d'anneaux Rasching. *Chem. Eng. Sci.* **1969**, *24*, 1097.

(42) Levich, V. G.; Markin, V. S.; Chismadzhev, Y. A. On hydrodynamic mixing in a model of a porous medium with stagnant zones. *Chem. Eng. Sci.* **1967**, *22*, 1357.

(43) Thompson, K. E.; Fogler, H. S. Modeling flow in disordered packed beds from pore-scale fluid mechanics. *AIChE J.* **1997**, *43*, 1377.

(44) Walsh, F. C.; Reade, G. Design and performance of electrochemical reactors of efficient synthesis and environmental treatment. Part 1. Electrode geometry and figures of merit. A*nalyst* **1994**, *119*, 791.

(45) Letord-Quémere, M. M.; Legrand, J.; Coeuret, F. Improvement of mass transfer in electrochemical cells by means of expanded materials. *Inst. Chem. Eng. Symp. Ser.* **1986**, *98*, 73.

(46) Ralph, T. R.; Hitchman, M. L.; Millington, J. P.; Walsh, F. C. Mass transport in an electrochemical laboratory filterpress reactor and its enhancement by turbulence promoters. *Electrochim. Acta* **1996**, *41*, 591.

(47) Goodridge, F.; Mamoor, G. M.; Plimley, R. E. *Inst. Chem. Eng. Symp. Ser.* **1986**, *98*, 61.

(48) Hammond, J. K.; Robinson, D.; Walsh, F. C. Mass transport studies in Filterpress Monopolar (FM-Type) Electrolysers I—Pilot scale studies in the FM21-SP reactor. *DECHEMA Monogr.* **1991**, *123*, 279.

(49) Hammond, J. K.; Robinson, D.; Walsh, F. C. Mass transport studies in Filterpress Monopolar (FM-Type) Electrolysers II—Laboratory studies in the FM01-LC reactor. *DECHEMA Monogr.* **1991**, *123*, 299.

(50) Brown, C. J.; Walsh, F. C.; Pletcher, D. Mass transfer and pressure drop in a laboratory filterpress electrolyser. *Trans. Inst. Chem. Eng.* **1995**, *73*, 196.

(51) Tagg, D. J.; Patrick, M. A.; Wragg, A. A. Heat and mass transfer downstream of abrupt nozzle expansions in turbulent flow. *Trans. Inst. Chem. Eng.* **1979**, *57*, 176.

(52) Wragg, A. A.; Tagg, D. J.; Patrick, M. A. Diffusion-controlled current distributions near cell entries and corners. *J. Appl. Electrochem.* **1980**, *10*, 43.

(53) Pickett, D. J.; Wilson, C. J. Mass transfer in a parallel plate electrochemical cell—the effect of change of flow area and flow cross-section at the cell inlet. *Electrochim. Acta.* **1982**, *27*, 591.

(54) Chouikhi, S. M.; Patrick, M. A.; Wragg, A. A. Mass transfer downstream of nozzles in turbulent pipe flow with varying Schmidt number. *J. Appl. Electrochem.* **1987**, *17*, 1118.

(55) Brown, C. J.; Pletcher, D.; Walsh, F. C.; Hammond, J. K.; Robinson, D. Local mass transport effects in FM01-LC laboratory electrolyser. *J. Appl. Electrochem.* **1992**, *22*, 613.

Received for review May 20, 1999
Revised manuscript received February 11, 2000
Accepted February 18, 2000

IE990351Q